Proceedings of the Society for

EXPERIMENTAL MECHANICS

Proceedings
of the Society
for

EXPERIMENTAL MECHANICS

(Formerly the Society for Experimental Stress Analysis)

VOLUME XLI

K.A. Galione, Publisher
M.E. Yergin, Editor

14 FAIRFIELD DRIVE
BROOKFIELD CENTER, CT 06805
Printed in U.S.A., 1984

Proceedings
of the Society
for Experimental
Mechanics

SEM Executive Board

President
W.N. SHARPE, JR.
The Johns Hopkins University

President-Elect
R.J. RINN
Measurements Group, Inc.

Vice-President
I.M. ALLISON
University of Surrey

Treasurer
D.L. WILLIS
Allison Gas Turbine
Division—GMC

Managing Director
K.A. GALIONE
SEM Headquarters

S.K. FOSS
John Deere Technical Center

W.L. FOURNEY
University of Maryland

A.S. KOBAYASHI
University of Washington

J.B. LIGON
Michigan Technological University

R.H. MARLOFF
Westinghouse R&D Center

S.E. SWARTZ
Kansas State University

W.M. MURRAY
Honorary President

Editorial Council

Chairman
R.J. RINN
Measurements Group, Inc.

Secretary
K.A. GALIONE
SEM Headquarters

D.A. DILLARD
University of Missouri

J.F. DOYLE
Purdue University

B.C. DYKES
The Boeing Company

S.K. FOSS
John Deere Technical Center

D.H. MORRIS
Virginia Polytechnic Institute
and State University

C.E. PASSERELLO
Michigan Technological University

J.W. PHILLIPS
University of Illinois

R.J. SANFORD
University of Maryland

D.L. WILLIS
Detroit Diesel Allison—GMC

W.N. SHARPE, JR.
The Johns Hopkins University
ex officio

Papers Review Committee

Chairman
D.H. MORRIS
Virginia Polytechnic Institute
and State University

D.B. BARKER
University of Maryland

C.W. BERT
University of Oklahoma

G.L. CLOUD
Michigan State University

C.W. HARRIS
Texas A&M University

W.H. PETERS III
University of South Carolina

P.K. STEIN
Stein Engineering Services, Inc.

J.L. TURNER
Auburn University

Notice: The opinions expressed on the following pages are those of the individual authors and do not necessarily represent the ideas of the Society for Experimental Mechanics.

Contents

Separation of Dynamically Induced Low-frequency Stresses in Rods and Pipes

Components of dynamically induced low-frequency stresses which propagate axially in opposite directions can be separated by measurements using fairly simple procedures

by Goran Pavić

ABSTRACT—Expressions are evaluated with which the separation of oppositely propagating axial-stress components in rods and pipes can be achieved from stress waveforms obtained at different locations on the rod or pipe. The corresponding measurement/processing procedures can produce either the power spectra or the waveforms of these components. Simplifications of basic procedures for waveform evaluation are formulated whenever possible.

A few experiments are described which verify the analytical results obtained theoretically and which also demonstrate the applicability of the separation procedures.

List of Symbols

Variables

A = amplitude spectral density of propagating stress waves
B = amplitude spectral density of decaying stress waves
c = velocity of wave propagation
d = axial distance
D = diameter
E = Young's modulus
f = frequency
i = imaginary unit $\sqrt{-1}$
k = wave number
l = gage length
n = integer
r = radius of inertia
s = pipe-wall thickness
S = power or cross-spectral density
t = time
T = averaging interval
u = arbitrary variable
U = amplitude
x = axial coordinate
α = flexural constant, eq (7)
β = constant, eq (8)
δ = gage to neutral axis distance
Δ = gage spacing
$\Delta\omega$ = frequency band
ϵ = error
η = lateral displacement
κ = shear coefficient
λ = wavelength
ν = Poisson's number
ξ = axial displacement
ϱ = mass density
σ = axial stress on measurement location
ω = angular frequency

Operators

F = Fourier transform
F^{-1} = Inverse Fourier transform
Im = imaginary part
Re = real part
$\overline{\ }$ = time-average value
$< >$ = spatial-average value
$\_$ = complex quantity
$\sim$ = approximate value

Indices

a = pertaining to a specific value
c = central
d = decaying
f = flexural
i = nonpropagating
l = longitudinal
m = middle
p = propagating
po = polar
y = axial
Δ = difference
$-$ = negative-propagating
$+$ = positive-propagating
0 = at position 0
1 = at position 1
2 = at position 2
$\rightarrow$ = pertaining to measured quantity
$\leftarrow$ = pertaining to nonmeasured quantity

Introduction

Dynamical stresses occur in rods and pipes when elastic waves take place. For a given rod (pipe) geometry, these waves assume definite spatial forms (modes) which are independent of the nature of wave excitation. The

Goran Pavic is Senior Research Fellow, Electrotechnical Institute "Rade Koncar", 41000 Zagreb, Bastijanova bb, Yugoslavia.

Original manuscript submitted: June 6, 1982. Final manuscript received: September 13, 1983.

spatial distribution and the time history of the excitation, however, determine the extent to which various modes are excited. As a consequence, some modes do not need to be excited at all.

Generally, two types of modes exist: propagating modes, which preserve the wave amplitudes and carry net mechanical energy, and nonpropagating modes, which have the opposite features. When changes in the excitation are not fast, i.e., at lower frequencies, two modes dominate the wave motion: simple extensional (longitudinal) and simple flexural modes. The term 'lower frequencies' applies to those frequencies at which the wavelengths are much larger than the lateral dimensions of the rod or pipe. The wave motion at lower frequencies takes place only in the axial direction.

The axial-wave motion in rods (pipes) of finite length always consists of two components traveling in opposite directions simultaneously due to the combined effect of primary wave generation and subsequent reflections at the terminations. Simple measurement of stresses can reveal only the total stress wave resulting from the superposition of the two oppositely transmitted components. In a number of situations, however, it would be advantageous to measure just one of the components, i.e., to perform a separation of the stress constituents. Such situations are encountered when problems of structure identification or diagnosis of stress origins arise.

A fairly simple yet sufficiently accurate procedure is described, by means of which the desired separation of the stress components can be achieved with the aid of easily available measuring equipment. The procedure is restricted to low-frequency stresses in uniform rods and pipes where only simple longitudinal and flexural modes are possible.

Stress-wave Representation

A general principle for the separation of wave components is described in Ref. 1. This principle is based on the assumption that the wave motion is strictly in the axial direction of a wave guide, and that for each frequency component of the wave there exists a definite, single-value real wave number. The wave number can depend on frequency in an arbitrary fashion, $k = k(\omega)$.

Wave motion at a single frequency is usually described in terms of complex amplitudes $\underline{U}_+$ and $\underline{U}_-$, corresponding to the + and − directions of propagation. The modulus of the complex amplitude, $|\underline{U}|$, is the actual physical amplitude. The quantity $\tan^{-1}\{Im\ \underline{U}/Re\ \underline{U}\}$ is the wave phase at the reference time instant $t = 0$:

$$\underline{u}(x,t) = \underline{U}_+ \exp[\,i(\omega t - kx)] + \underline{U}_- \exp[i(\omega t + kx)]$$

The physically realistic wave motion is simply the real part of $\underline{u}$, $u = Re\{\underline{u}\}$.

Generally, the time histories of stress waves are not harmonic. Expressed in terms of its frequency composites, the total stress wave, being the sum of two opposite-traveling components σ_+ and σ_-, reads:

$$\sigma(x,t) = \sigma_+(x,t) + \sigma_-(x,t) \tag{1}$$

where

$$\begin{aligned}\sigma_+(x,t) &= \int_0^\infty Re\{\underline{A}_+(\omega)\exp[i(\omega t - kx)]\}d\omega \\ \sigma_-(x,t) &= \int_0^\infty Re\{\underline{A}_-(\omega)\exp[i(\omega t + kx)]\}d\omega\end{aligned} \tag{2}$$

$\underline{A}_+$ and $\underline{A}_-$ are the stress (complex) amplitude densities. This means that an elementary-frequency constituent of the stress, occupying an elementary-frequency width $d\omega$ at some frequency ω_a, has the amplitude $|\underline{A}(\omega_a)|d\omega$ and the phase $\tan^{-1}[Im\ \underline{A}(\omega_a)/Re\ \underline{A}(\omega_a)]$.

The assumption of real wave numbers incorporated in eq (2) implies the existence of propagating modes only. To account for the possibility of nonpropagating modes, two additional stress components, σ_{+i} and σ_{-i}, are introduced.

$$\begin{aligned}\sigma_{+i}(x,t) &= \int_0^\infty Re\{\underline{B}_+(\omega)\exp[i\omega t - kx]\}d\omega \\ \sigma_{-i}(x,t) &= \int_0^\infty Re\{\underline{B}_-(\omega)\exp[i\omega t + kx]\}d\omega\end{aligned} \tag{3}$$

These are characterized by imaginary wave numbers (Ref. 2, section 3.1) which correspond to the decaying modal pattern of these components. The component σ_{+i} decays in the positive axial direction. The component σ_{-i} decays in the negative direction. The quantities $\underline{B}_+(\omega)$ and $\underline{B}_-(\omega)$ are the amplitude densities of the nonpropagating components at the reference position $x = 0$.

If $\underline{U}(\omega)$ is the Fourier transform of a real function of time $u(t)$ (Ref. 3, section 3.1), then

$$\underline{U}(\omega) = F\{u(t)\} = \int_{-\infty}^{\infty} u(t)\exp(-i\omega t)dt$$

Its inverse, $F^{-1}\{\underline{U}(\omega)\} = u(t)$, can be obtained by the integration over positive frequencies only:

$$F^{-1}\{\underline{U}(\omega)\} = \frac{1}{2\pi}\int_{-\infty}^{\infty}\underline{U}(\omega)\exp(i\omega t)d\omega = \frac{1}{\pi}\int_0^\infty Re[\underline{U}(\omega)\exp(i\omega t)]d\omega$$

Since eqs (2) and (3) hold identically for any t and ω, it follows that the Fourier transforms of the stress components are

$$\begin{aligned}F\{\sigma_+(x,t)\} &= \pi\underline{A}_+\exp(-ikx), & \sigma_+ &= \sigma_{p+} \\ F\{\sigma_-(x,t)\} &= \pi\underline{A}_-\exp(ikx), & \sigma_- &= \sigma_{p-} \\ F\{\sigma_{+i}(x,t)\} &= \pi\underline{B}_+\exp(-kx), & \sigma_{+i} &= \sigma_{d+} \\ F\{\sigma_{-i}(x,t)\} &= \pi\underline{B}_-\exp(kx), & \sigma_{-i} &= \sigma_{d-}\end{aligned} \tag{4}$$

Relations (4) form the basis for the formulation of the separation procedure.

Wave Numbers at Low Frequencies

The simple, 'classical', wave equation for homogeneous thin rods yields a simple wave number - frequency dependence for longitudinal mode (Ref. 2, section 2.5):

$$k = \omega/c_l \qquad c_l = \sqrt{E/\varrho} \tag{5}$$

It is based on the assumption of uniform stress distribution over the cross section and does not account for the effects of inertia caused by lateral contraction. If these effects are included into the calculation (still assuming the uniform stress distribution), a cross term called Rayleigh's correction appears in the wave equation, resulting in a dispersive k-ω dependence (Ref. 2, section 2.5):

$$k = \frac{\omega/c_\ell}{\sqrt{1 - (\nu r_{po})^2(\omega/c_\ell)^2}} \tag{6}$$

A five-percent deviation from eq (6) can be used as the practical limit of the ability of eq (5) to determine the upper frequency:

$$f_u \simeq \frac{1}{20}\,\frac{c_\ell}{\nu r_{po}}$$

Consequently the lowest wavelength below which eq (5) is not usable is determined by the following relationship:

$$\frac{\lambda}{r_{po}} \simeq 20\,\nu$$

In other words, for circular solid rods of diameter D ($r_{po} = D/2\sqrt{2}$), the simple - dependence eq (5) is sufficiently accurate, providing the wavelength exceeds $\sim 7\,\nu D$. For metal rods, this limit is twice the diameter. The same five-percent criterion applied to pipes [$r_{po} = \frac{1}{2} D_m\sqrt{1 + S/D_m)^2}$] gives $\lambda > 10\,\nu D_m$. Thus for metal pipes, the wavelength must be at least three times the mean diameter.

To obtain an exact solution of the governing equation for longitudinal wave propagation in rods (and thus an exact k-ω dependence), the assumption of uniform stress distribution must be abandoned. The type of solution then depends on the shape of the cross section. For example in the case of a circular solid rod, the wave number is given in terms of a combination of Bessel functions (Pochhammer frequency equation, Ref. 2, section 8.2).

An exact solution for flexural wave propagation also depends on the shape of the cross section of the rod (pipe). It turns out that an unlimited number of modes are possible for both the longitudinal and flexural motions. The lowest mode, however, is associated with the low-frequency behavior as defined previously. This behavior is described for flexural waves with a simple but dispersive dependence (Ref. 2, section 3.1):

$$k = \alpha\sqrt{\omega} \quad \text{or} \quad k = i\,\alpha\sqrt{\omega}$$
$$\alpha = \frac{1}{\sqrt{r_y c_\ell}} \tag{7}$$

The real wave number corresponds to propagating waves, while the imaginary wave number corresponds to decaying waves.

Several simplifying assumptions were employed to obtain an equation of motion corresponding to eq (7): (a) the strains in a rod subjected to flexure rise linearly from the neutral axis (passing through the centroid of the cross section), (b) the curvature of the rod is always small and (c) the effects of rotary inertia and cross-sectional shear are negligible. If the rotary inertia and cross-sectional shear are taken into account, a solution for the wave number - frequency dependence is obtained as (Ref. 2, section 3.4):

$$k = \frac{1}{r_y}\sqrt{\frac{\omega r_y}{c_\ell}\sqrt{1 + \left(\frac{1-\beta}{2}\right)^2\left(\frac{\omega r_y}{c_\ell}\right)^2} + \frac{1+\beta}{2}\left(\frac{\omega r_y}{c_\ell}\right)^2}$$
$$\beta = \frac{2(1+\nu)}{\varkappa} \tag{8}$$

which is in very good agreement with an exact solution based on a rigorous application of the theory of elasticity. The shear coefficient $\varkappa$ depends on the cross section. For example, it is 1.11 for a circular cross section.

The wave number k given by eq (8) tends toward the value $\sqrt{\omega/r_y c_\ell}$ given by eq (7) where $\omega r_y/c_\ell \to 0$. At low frequencies where $\omega r_y \ll c_\ell$, an approximation can be derived from eq (8):

$$k = \frac{1}{r_y}\sqrt{\frac{\omega r_y}{c_\ell} + \frac{1+\beta}{2}\left(\frac{\omega r_y}{c_\ell}\right)^2} \approx \sqrt{\frac{\omega}{r_y c_\ell}}\left(1 + \frac{1+\beta}{4}\,\frac{\omega r_y}{c_\ell}\right)$$

by means of which a criterion can be established for the applicable limit of eq (7). If the five-percent accuracy margin is invoked, the frequency below which the simplified-dependence eq (7) is acceptable becomes:

$$f_u \approx \frac{0{,}1\,\varkappa}{\pi[\varkappa + 2(1+\nu)]}\,\frac{c}{r_y}$$

and the corresponding minimum λ/r_y ratio reads:

$$\frac{\lambda}{r_y} = \frac{2\pi}{k r_y} \approx 2\pi\sqrt{\frac{\varkappa + 2(1+\nu)}{0{,}2\,\varkappa}}$$

In other words for circular metal rods ($r_y = D/4$), the minimum wavelength to diameter ratio should be 6,42 if eq (7) is to be within the five-percent limit.

In the rest of the analysis of dealing with practical measurement procedures, the validity of eqs (5) and (7) is assumed. In no way, however, should these procedures be restricted only to the low-frequency region if more accurate k-ω laws are accounted for. The only necessary condition concerning their applicability is the occurrence of wave motion in one axial mode.

Separation Procedure

At the present it is assumed that only propagating components are contained in the wave motion. This assumption, which is always valid for the longitudinal mode at low frequencies, becomes realistic for the flexural mode if the measurement location is a sufficient distance (a couple of wavelengths) away from the terminations. If this last condition is not fulfilled, a procedure described in Appendix A may be employed to separate in measurements the propagating from the nonpropagating wave components.

From eq (4) and the linear properties of Fourier-transform (FT) and differentiation operations, the following relationships are obtained for the FT of the stress spatial derivative $\partial\sigma/\partial x$.

$$F\left\{\frac{\partial}{\partial x}\,\sigma\right\} = F\left\{\frac{\partial}{\partial x}\,\sigma_+\right\} + F\left\{\frac{\partial}{\partial x}\,\sigma_-\right\} =$$
$$ik(-F\{\sigma_+\} + F\{\sigma_-\})$$

By taking the inverse transform of the last expression divided by $-ik$, an expression for the difference of the stress components is reached.

$$F^{-1}\left\{\frac{i}{k}\,\frac{\partial\sigma}{\partial x}\right\} = \sigma_+ - \sigma_- \tag{9}$$

This expression makes their separation possible, providing the stress gradient $\partial\sigma/\partial x$ is measured simultaneously with the stress σ itself.

$$\sigma_{\pm} = \frac{1}{2}\left[\sigma \pm F^{-1}\left(\frac{i}{k} F\left\{\frac{\partial \sigma}{\partial x}\right\}\right)\right] \qquad (10)$$

Stresses are detected by measurement of strains. Strain-gradient-sensitive transducers are not available. The necessity for measurement of $\partial\sigma/\partial x$ leads to an application of finite-difference approximations:

$$\frac{\partial \sigma}{\partial x} \approx \frac{1}{\Delta}\left[\sigma(x + \Delta/2, t) - \sigma(x - \Delta/2, t)\right] = \frac{1}{\Delta}(\sigma_2 - \sigma_1)$$

$$\Delta \ll \qquad (11)$$

The stress gradient is thus replaced by the difference of stresses measured at two closely spaced points, 1 and 2, located symmetrically about the reference position. It will be shown that the accuracy of the approximation of eq (11) depends on the value of product $k\Delta$; the smaller this product the higher the accuracy.

Denoting the measurement locations by 0, 1 and 2 as shown in Fig. 1, eq (10) takes an alternative form:

$$\tilde{\sigma}_{\pm} = \frac{1}{2}\sigma_0 \pm \frac{1}{2\Delta} F^{-1}\left(\frac{i}{k} F\{\sigma_2 - \sigma_1\}\right) \qquad (12)$$

which will serve as a basis for the stress-separation procedure.

Bridge Arrangements

Measurement of stresses (i.e., strains) at three locations as required by eq (12) is simply achieved by use of ordinary strain gages wired into appropriate conditioning bridges. Two gages are needed at each location (if longitudinal and flexural motion exist at the same time), and should be placed symmetrically about the neutral axis of the rod (pipe). In this way the stresses can be detected, induced either by the axial component of the motion or by the flexural component. The sum of the strain equals the double compression-induced stress component divided by the Young's modulus, while the strain difference equals the double flexure-induced stress divided by the Young's modulus.

Figure 2 shows schematically the gage connections necessary for the separation procedure based on the finite-difference approach. It can be seen that in both cases the four outer gages are connected in a full-bridge configuration, while the two middle gages are connected in a half-bridge requiring two additional completion resistors.

When only one of the motions exists (either longitudinal or flexural), there is no necessity for two gages at each location—one gage per location is sufficient. In that case the corresponding bridge configurations are half-bridge for the outer gages and quarter-bridge for the middle gage.

Practical Measurement Procedures: Spectral Densities

Equation (12) is not suitable for use in its direct form. To implement this equation in any practical case, the Fourier-transform (FT) operation has to be applied twice—once direct, once inverse—to the measured data. This necessitates the use of a signal analyzer which incorporates a FT program. The analyzers available can perform FT procedure over a very limited length of data. Short-duration transients only can be processed in the way indicated by eq (12).

The power-spectral-density functions (PSD) of the components $\tilde{\sigma}_+$ and $\tilde{\sigma}_-$ can be evaluated, however, without limitations in all the cases where the stresses are of random nature. By applying the definition of and the addition laws for the PSD functions (Ref. 3, section 9.1), the power-spectrum densities of the components $\tilde{\sigma}_+$ and $\tilde{\sigma}_-$ are found to be

$$S\tilde{\sigma}_{\pm}(\omega) = \frac{1}{4} S\sigma_0(\omega) + \frac{1}{4\Delta^2 k^2(\omega)} S\sigma_\Delta(\omega) \mp \frac{1}{2\Delta k(\omega)} Im\left\{\underline{S}\sigma_0\sigma_\Delta(\omega)\right\} \qquad (13)$$

σ_Δ stands for the stress difference $\sigma_\Delta = \sigma_2 - \sigma_1$.

The PSD function of either of the stress components is seen to be a linear combination of the PSD of the total stress, $S\sigma_0$, the weighted PSD of the stress difference, $S\sigma_\Delta$, and the weighted cross-spectral-density function between the total and the difference stresses, $\underline{S}\sigma_0\sigma_\Delta$. Each of these three spectral densities can be evaluated separately on a signal analyzer.

The mean-square values, and thus the RMS values, of the components $\tilde{\sigma}_+$ and $\tilde{\sigma}_-$ are easily obtained from the PSD functions by integration (Ref. 3, section 9.1)

$$\overline{\tilde{\sigma}_{\pm}(t)^2} = \lim_{T\to\infty} \frac{1}{2T} \int_{-T}^{T} \tilde{\sigma}_{\pm}(t)^2\, dt = \frac{1}{\pi} \int_0^{\infty} S\tilde{\sigma}_{\pm}(\omega)\, d\omega \qquad (14)$$

Practical Measurement Procedures: Waveforms

The waveform of either of the stress components, generated by longitudinal wave motion, can be obtained from measurements without any transformation procedure owing to the nature of the corresponding k-ω dependence. Since $F\{u(t)\}/i\omega = F\{\int u(t)dt\}$, it follows that the separation of compression-induced stresses requires simply an integration operation instead of double integral transformation:

$$\tilde{\sigma}^l_{\pm} = \frac{\sigma^l_0}{2} \mp \frac{c_l}{2\Delta} \int \sigma^l_\Delta(t)\, dt \qquad (15)$$

Such an integration can be easily accomplished by use of an analog electronic circuit during the measurement process.

This simple separation procedure is not applicable to flexure-induced stresses unless narrow-band frequency measurements are made. In the latter case, the following approximation holds.

$$F^{-1}\left\{\frac{i}{k} F\,\sigma_\Delta\right\} \approx \frac{\sqrt{\omega_c}}{\alpha} F^{-1}\left\{\frac{i}{\omega} F\,\sigma_\Delta\right\} = -\frac{\sqrt{\omega_c}}{\alpha} \int \sigma_\Delta(t)\, dt$$

The separation becomes governed by a formula analogous to eq (15):

$$\tilde{\sigma}^f_{\pm} = \frac{\sigma^f_0}{2} \mp \frac{\sqrt{\omega_c}}{2\alpha\Delta} \int \sigma^f_\Delta(t)\, dt \qquad (16)$$

This formula is valid only if the center frequency of the band, ω_c, considerably exceeds the effective band width,

$\Delta\omega$, i.e., if $|\omega - \omega_c| \ll \omega_c$ throughout the effective band range.

For the case of broad-band measurements of flexure-induced stress components, no simplifications are possible, and the separation must be conducted on the basis of eq (12).

An alternative to the procedure based on eq (15) is to measure the velocity of wave motion instead of stress difference. The equilibrium equation for longitudinal wave motion (Ref. 2, section 2.1),

$$E\frac{\partial^2\xi}{\partial x^2} = \frac{\partial\sigma^\ell}{\partial x} \equiv \varrho\frac{\partial^2\xi}{\partial t^2}$$

is simply substituted into eq (15) where $\sigma^\ell_\Delta/\Delta$ corresponds to $\partial\sigma^\ell/\partial x$ to give an exact (not any more approximate) expression for the components σ_+ and σ_-.

$$\sigma^\ell_\pm = \frac{\sigma^\ell_0}{2} \mp \frac{c_\ell\varrho}{2}\frac{\partial\xi}{\partial t} \tag{17}$$

Thus instead of measuring the stress difference between 2 and 1, the longitudinal velocity at 0 can be measured in order to obtain the two stress components. The last type of measurement is probably more convenient when dealing with compression-induced stresses since it neither comprises approximations nor requires any time integration. It could however prove difficult to find velocity transducers which are sensitive enough to satisfy the requirements of such measurements.

Measurement Accuracy

There are various sources of inaccuracies accompanying practical measurements based on eq (12). The most important of these sources arise due to finite spacing between strain gages, finite length of the gages and instrumentation noise.

—The difference of stresses, $\sigma_2 - \sigma_1$, divided by the gage spacing, Δ, is only an approximation of the stress gradient $\partial\sigma/\partial x$.

—Strain gages which have to be used in measurements are of finite length and consequently detect an average value of stress along their length instead of detecting the stress at one specific point.

—There is always unwanted electrical noise in measuring equipment which contaminates readings.

The first two of these sources produce a measurement bias, while the third one creates random error.

The measurement bias is examined in Appendix B. It has been found that this quantity is frequency dependent. The bias in measurement of compression-induced components increases with the square of frequency, while measurements of flexure-induced components produce bias which rises linearly with frequency. The method described underestimates the component being measured (factor ϵ_{--} in Appendix B) and is subjected at the same time to the influence of the other stress component (factor ϵ_{-+}).

Under normal circumstances the gage length will be much smaller than the gage spacing, Δ. Thus if condition $k\Delta \leq 1$ is ensured, the measurement accuracy will be sufficient for most practical purposes (<two-percent error). Too small values of $k\Delta$ are not convenient either: the smaller the $k\Delta$, the smaller the output signal from the gage bridge measuring σ_Δ, and consequently the smaller the signal-to-noise ratio. Therefore, an optimum spacing should be adjusted for each particular measurement to produce the bias comparable to the signal-to-noise ratio.

Experimental Results

Following the separation technique described, a few experiments were carried out on a 4.7-m long copper pipe of 25-mm diameter and 4-mm wall thickness. The measurement location was 1.4 m away from one of the ends. The gage spacing was Δ = 200 mm.

During the measurements the end of the pipe opposite to the measurement location was either free or rigidly attached to a steel plate, 1.8 m², damped with an anti-vibration coating. In this way two different boundary conditions were achieved on this end: one without and one with a loss of energy. The rigid attachment ensured a complete transfer of the pipe motion to the plate, both for longitudinal and flexural motions. Figure 3 shows a schematic layout of the pipe with the plate.

The pipe was excited at the end nearer to the measurement area. At this end the pipe was flattened and then

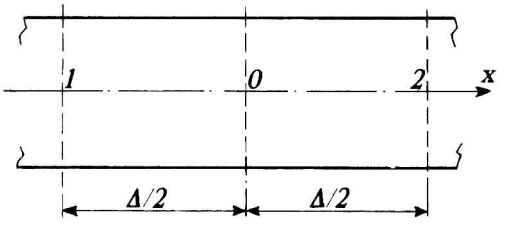

Fig. 1—Measurement locations on a rod (pipe)

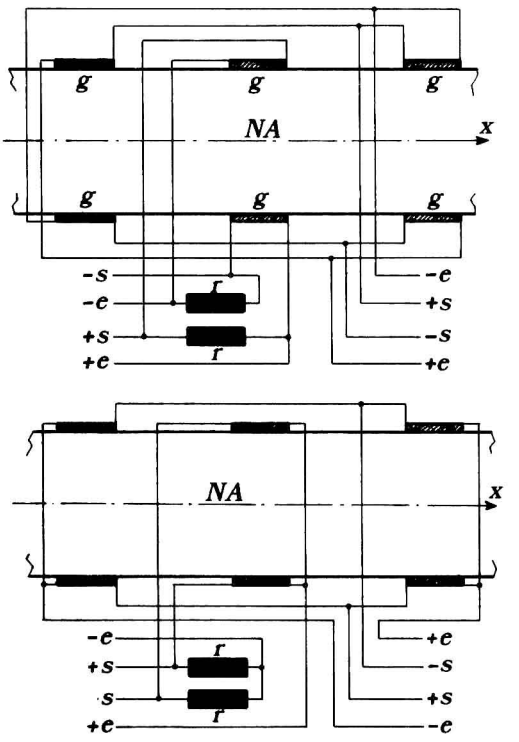

Fig. 2—Strain-gage bridges for measurement of compression-induced stresses (above) and flexure-induced stresses (below).

s = signal, *e* = excitation, *g* = strain gage, *r* = completion resistor, *NA* = neutral axis

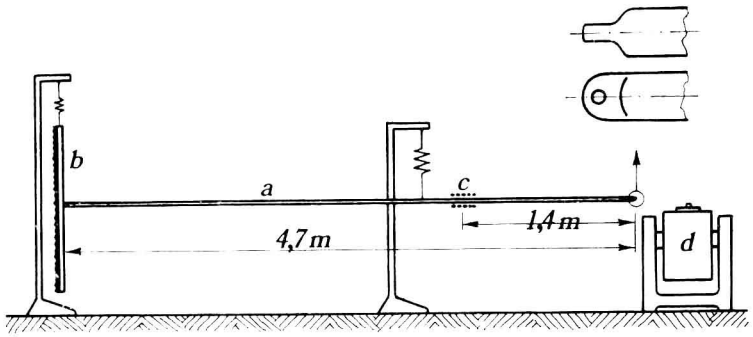

Fig. 3—Measurement of stress components on a pipe.
a = pipe, *b* = damped plate, *c* = strain-gage bridge (Micro Measurements CEA-06-250 UW-120), *d* = electrodynamic vibrator (Ling Dynamics 712). Upper-right corner depicts side and top view of pipe termination

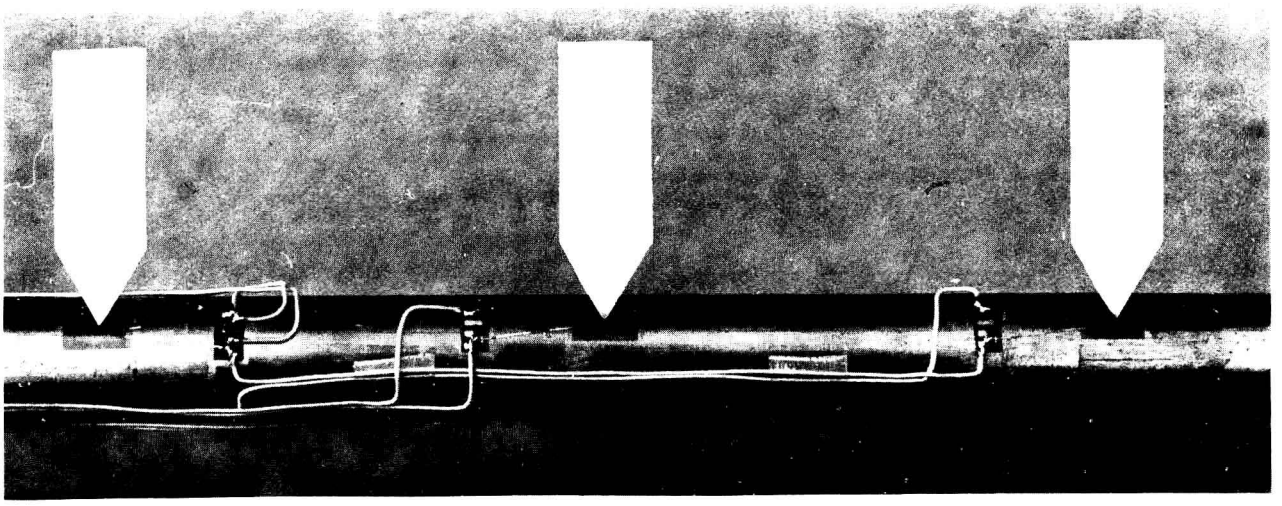

Fig. 4—Strain-gage bridges on pipe. Gages are indicated by arrows

rounded as shown in Fig. 3. In this way it became possible to apply force either in the axial direction (for excitation of longitudinal waves), or in the lateral direction (for flexural waves). The same gages were used for measurements of compression and flexure-induced stresses, but different bridges were formed in each case by choosing the corresponding wiring scheme from Fig. 2. Figure 4 reveals details of the measurement bridge wired for compression-induced stress-component detection.

Integration, summation and differentiation of signals, according to eqs (15) and (16), were done electronically using custom-built analog circuits based on operational amplifiers. In addition to the basic operation for evaluating $\tilde{\sigma}_+$ and $\tilde{\sigma}_-$, bandpass electronic filtering of measured signals was included when measuring waveforms. The objective of filtering was to extract only the desired frequency portions of stresses from the total stress time histories. The filters used were tightly matched both in amplitude and phase characteristics, which is essential when comparing waveforms. The measurement setup used is shown in Fig. 5.

Figures 6, 7, 8 and 9 show the waveforms of $\tilde{\sigma}_+^l$, $\tilde{\sigma}_-^l$ and the quantities which contribute to them obtained by a single hammer blow in the axial direction at the excitation point of the pipe. The abscissa origin, $t = 0$, coincides with the beginning of the impact. In one case (Figs. 6 and 7) the filtering was broadband. In the other (Figs. 8 and 9) it was medium band. Note that in cases without damping, the stress component $\tilde{\sigma}_-^l$ is just the inverse replica of $\tilde{\sigma}_+^l$ shifted by a certain time interval. This interval equals the travel time of stress from the measurement position to the opposite end and back the same way with the velocity c_l (which was 3775 ms^{-1} for the material used). The change of sign in $\tilde{\sigma}_-^l$ is the result of the conditions at the force-release boundary. In cases with damping, a noticeable change between the outgoing and returning stress components can be observed. Comparison of Fig. 7 to Fig. 9 indicates that this change is predominantly due to more efficient absorption of higher frequency components of stresses.

Figure 10 shows the same quantities as the previous four figures, but obtained with a transversely applied hammer impact producing flexure-induced stresses. The damping plate was disconnected in this experiment. The signals were passed through narrow, 150-250 Hz, bandpass filters to make the simplified separation procedure [eq (16)] applicable. The characteristic delay interval between $\tilde{\sigma}_-^l$ and $\tilde{\sigma}_+^l$ corresponds to the group velocity of flexural waves at the band-center frequency (200 Hz), which in the given case equals 405 ms^{-1} ($c_g = 2\omega/k$).

The pipe with free ends necessarily contains decaying stress components in flexural wave motion. These have an amplitude at the ends which equals the amplitudes of propagating wave components (Ref. 2, section 3.1). Un-

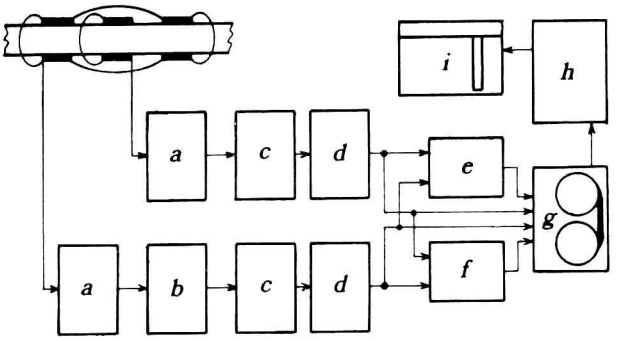

Fig. 5—Instrumentation setup.
a = bridge-conditioning amplifier (Honeywell Accudata 218), *b* = integrator, *c* = low-pass filter (Precision Filters LP 616), *d* = high-pass filter (Precision Filters HP 616), *e* = summation amplifier, *f* = difference amplifier, *g* = instrumental tape recorder (Honeywell 101), *h* = digital-event recorder (Bruel Kiaer 7502), *i* = x/y plotter (Hewlett-Packard 7004 B)

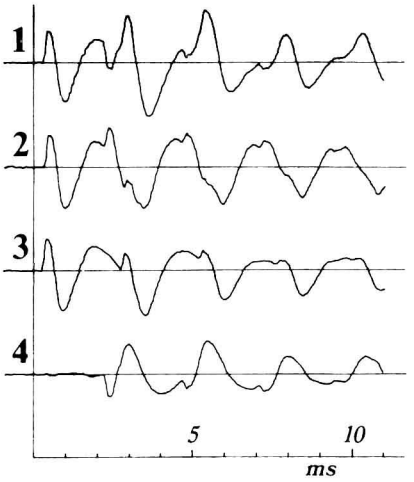

Fig. 7—Same as Fig. 6 for pipe attached to damped plate

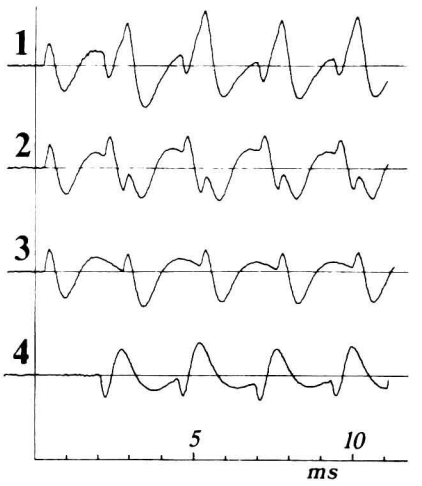

Fig. 6—Longitudinal, broadband (200-6000 Hz) stress components in free pipe: (1) σ^{ℓ}, (2) $\frac{-c_{\ell}}{\Delta}\int \sigma_{\Delta}^{\ell} dt$, (3) $\tilde{\sigma}\downarrow^{\ell}$, (4) $\tilde{\sigma}\downarrow^{\ell}$

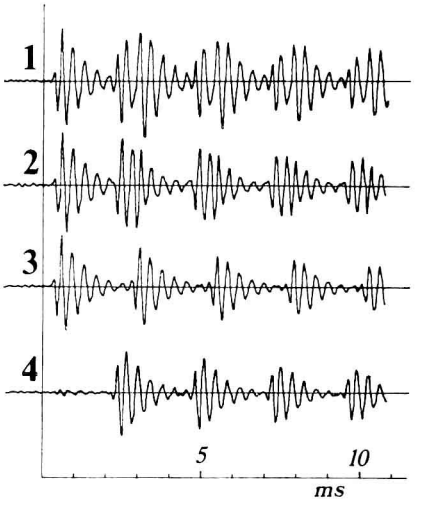

Fig. 8—Same as Fig. 6 for 2.5-6 kHz frequency band (free pipe)

like the amplitude of a traveling component which is constant, the amplitude of a decaying component decreases by a factor e^{-kd} with the distance d from the end. In the case considered, the decaying components at the measurement location were an average of $e^{8.59} \approx 5000$ times smaller from the propagating ones (−54 dB), and thus gave practically no contribution to the results.

Figures 11 and 12 show the PSD functions of flexure-induced stresses produced by a shaker attached to the excitation point and driven by random excitation of constant spectral density. The spectra were evaluated by an FFT analyzer, using eq (13). The peaks in the $\tilde{\sigma}_{+}^{f}$ spectrum indicate pipe resonances, which differ for the cases with and without the plate as the attached plate changes the dynamic properties of an otherwise free pipe.

The ratio of the $\tilde{\sigma}_{+}^{f}$ and $\tilde{\sigma}_{-}^{f}$ PSD's for undamped pipe-end condition closely approaches the theoretically expected value of 1. The same ratio displays a frequency dependence after attaching the plate and is always positive as expected. Two pronounced peaks can be observed on this plot. The plate itself has resonances at 158 and 248 Hz (detected from a separate plate moment-impedance measurement) which explains the two peaks. This coincidence simply indicates that a major energy transfer from the undamped pipe to the damped plate occurs only in the vicinity of the plate resonances. Such a conclusion is well supported by theoretical consideration of energy transfer from a force-type source of excitation.

Conclusions

Implementing the method for separation of low-frequency, oppositely propagating stress components in rods and pipes does not appear difficult. Power spectral densities of these components can be evaluated from measurements for any of the stress-wave types. Stress waveforms, however, can be detected in a much simpler way for compression-induced stresses than for flexure-induced ones. Simple detection of the latter is restricted

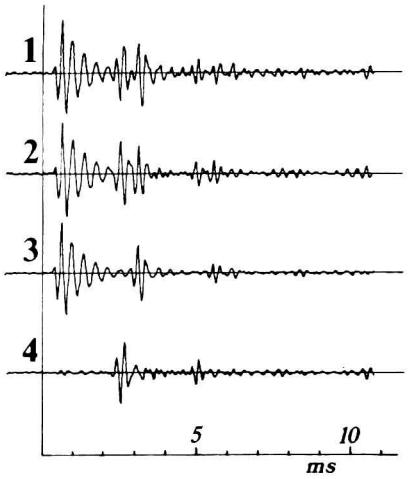

Fig. 9—Same as Fig. 8 for pipe attached to damped plate

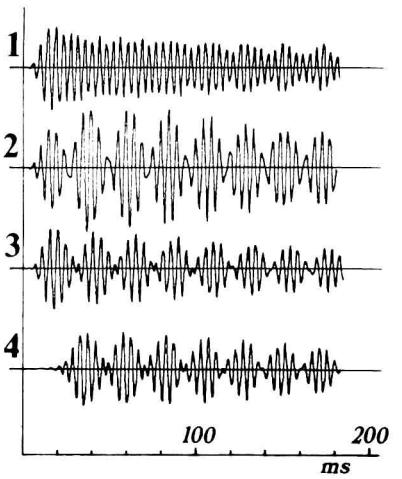

Fig. 10—Flexure-induced stress components in 150-250 Hz frequency band (free pipe): (1) σ^f, (2) $\frac{-\sqrt{\omega_c}}{\Delta\alpha}\int \sigma_\Delta^f\,dt$, (3) $\bar{\sigma}_+^f$, (4) $\bar{\sigma}_-^f$

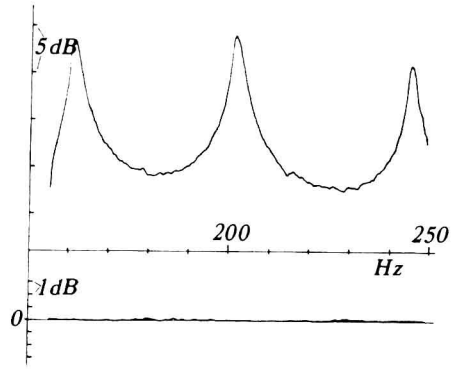

Fig. 11—Power spectrum of flexure-inducec stress in free pipe: (1) $S\,\bar{\sigma}_+ f$, (2) $S\,\bar{\sigma}_+ f/S\,\bar{\sigma}_- f$

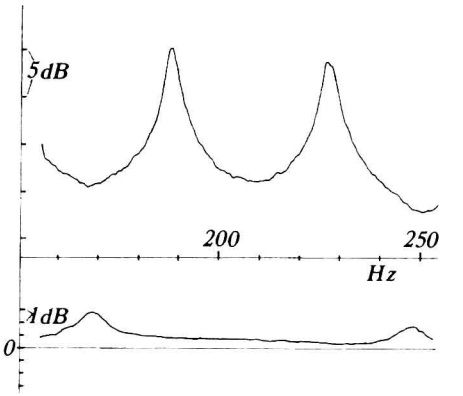

Fig. 12—Same as Fig. 11 for pipe attached to damped plate

to narrow-band measurement conditions only. Experiments demonstrate that ordinary equipment is sufficient for the majority of possible applications of the proposed method.

References

1. Pavić, G., "Separation of Structural Wave Components," Proc. Inst. Acoustics Spring Conf., Newcastle upon Tyne, Paper 14A3, 71-74 (1981).
2. Graff, K., "Wave Motions in Elastic Solids," Clarendon Press, Oxford (1975).
3. Papoulis, A., "Signal Analysis," McGraw-Hill, New York (1977).

APPENDIX A: Suppression of Decaying Stress Components

In a general case of flexural motion of a pipe, the total stress consists not only of the propagating components, σ_p^f, $\sigma_p^f = \sigma_{p+}^f + \sigma_{p-}^f$, but also contains the decaying components, σ_d^f, $\sigma_d^f = \sigma_{d+}^f + \sigma_{d-}^f$. The Fourier transform of the total stress is related in this case to the amplitude spectral densities of the propagating $\underline{A}(\omega)$ and decaying $\underline{B}(\omega)$ contributions as [eq (4)]

$$F\{\sigma^f(t)\} = \pi(\underline{A}_+ e^{-ik_f x} + \underline{A}_- e^{ik_f x} + \underline{B}_+ e^{-k_f x} + \underline{B}_- e^{k_f x}) = \pi(\underline{A} + \underline{B}) \quad \text{(A1)}$$

By differentiating eq (A1) twice with respect to x, propagating terms change sign in relation to decaying ones. This enables cancellation of the decaying terms by an appropriate arithmetic manipulation:

$$\sigma_p^f = \frac{\sigma^f}{2} - F^{-1}\left\{\frac{1}{2k_f^2} F\left(\frac{\partial^2 \sigma^f}{\partial x^2}\right)\right\} \quad \text{(A2)}$$

The expression, corresponding to eq (10) but applicable when σ_d stresses are present, reads

$$\sigma_{p_\pm}^f = \frac{\sigma^f}{4} + \frac{1}{4} F^{-1}\left\{\sum_{n=1}^{3} \left(\pm \frac{i}{k_f}\right)^n F\left(\frac{\partial^n \sigma^f}{\partial x^n}\right)\right\} \quad \text{(A3)}$$

If a finite-difference technique similar to the one used in eq (12) is to be employed to convert eq (A3) into a usable form, seven instead of three measurement locations would be needed as the highest spatial derivative in eq (A3) is for

two orders higher. Practical realization of measurements would become difficult with such a technique. Here is a simpler technique which does not necessitate any measurements of higher order derivatives.

The equilibrium equation for low-frequency flexural motion of a pipe (Ref. 2, section 3.1),

$$-\frac{\partial^4\eta}{\partial x^4} = \alpha^4\frac{\partial^2\eta}{\partial t^2}$$

transformed with the aid of the stress-curvature relationship

$$\sigma^f = -\delta E\frac{\partial^2\eta}{\partial x^2}$$

leads to a simple expression:

$$\frac{\partial^2\sigma^f}{\partial x^2} = E\delta\alpha^4\frac{\partial^2\eta}{\partial t^2} \tag{A4}$$

This expression relates the second spatial derivative of the total stress in the pipe to the lateral acceleration. As a consequence, eq (A2) with the aid of eq (A4) transforms into a linear stress-velocity combination:

$$\sigma_p^f = \frac{\sigma^f}{2} - \frac{D\alpha^2}{2}F^{-1}\left\{iF\left(\frac{\partial\eta}{\partial t}\right)\right\} \tag{A5}$$

Thus the measurement of the propagating portion of the flexure-induced stresses can be achieved by measurement of the stress and the lateral velocity at one location only. Finally, to separate out one of the propagating components, the finite-difference procedure of the type of eq (11) should be applied after substituting σ_p^f instead of σ in eq (12).

$$\tilde{\sigma}_{p\pm}^f = \frac{\sigma_0^f}{4} \pm \frac{1}{4\Delta\alpha}F^{-1}\left\{\frac{i}{\sqrt{\omega}}F(\sigma_2^f - \sigma_1^f)\right\} -$$

$$+\frac{E\delta\alpha^4}{4}F^{-1}\left\{-iF\left(\frac{\partial\eta_0}{\partial t}\right) \pm \frac{1}{\Delta\alpha\sqrt{\omega}}F\left(\frac{\partial\eta_2}{\partial t} - \frac{\partial\eta_1}{\partial t}\right)\right\} \tag{A6}$$

The use of the stress-component representation, eq (A1), can be further extended by evaluating expressions for the total stress component in one direction, e.g., + direction.

$$\tilde{\sigma}_+^f = \tilde{\sigma}_{p+}^f + \sigma_{d+}^f = \frac{\sigma_0^f}{2} \mp \frac{1}{4\Delta\alpha}F^{-1}\left\{\frac{1-i}{\omega}F(\sigma_2^f - \sigma_1^f)\right\}$$

$$\mp\frac{E\delta\alpha}{4\Delta}F^{-1}\left\{\frac{1+i}{\sqrt{\omega}}F\left(\frac{\partial\eta_2}{\partial t} - \frac{\partial\eta_1}{\partial t}\right)\right\} \tag{A7}$$

Note that both eqs (A6) and (A7) require double transforms. Simplifications can again be achieved if narrow-band measurements are taken. In this case the frequency ω is replaced by a constant, the band center frequency, ω_c. The imaginary unit, which also appears in eqs (A6) and (A7) is conveniently dealt with in one of the following ways.

$$i \approx \frac{i\omega}{\omega_c} \rightarrow \frac{1}{\omega_c}\frac{d}{dt}$$

$$i \approx -\frac{\omega_c}{i\omega} = -\omega_c\int(\,)\,dt$$

These expressions convert its operation in frequency domain into either differentiation or integration in the time domain, as was done to obtain eq (16).

APPENDIX B: Measurement Bias

The relationship between the amplitude spectral densities of the propagating stress components, $\sigma_+(t)$ and $\sigma_-(t)$, and the Fourier transform of the total stress, $\sigma(t) = \sigma_+(t) + \sigma_-(t)$, follows from eq (A1) after replacing σ^f by σ and equating $\underline{B}_+$ and $\underline{B}_-$ to zero.

The output signal from a strain gage is proportional to the mean value of the stress along the gage length.

$$<\sigma(t,x)> = \frac{1}{l}\int_{x-l/2}^{x+l/2}\sigma(t,x)dx$$

By putting $x = 0$ for the location 0, the Fourier transforms of the stress difference at 2 and 1, and of the stress at 0—as detected by the gages—read:

$$F\{\sigma_2 - \sigma_1\} = \frac{\pi}{l}\left[\int_{\Delta/2-l/2}^{\Delta/2+l/2}(\underline{A}_+e^{-ikx} + \underline{A}_-e^{ikx})\,dx -\right.$$

$$\left.-\int_{-\Delta/2-l/2}^{-\Delta/2+l/2}(\underline{A}_+e^{-ikx} + \underline{A}_-e^{ikx})dx\right] =$$

$$-2\pi i\frac{\sin(kl/2)}{kl/2}\sin(k\Delta/2)(\underline{A}_+ - \underline{A}_-)$$

$$F\{\sigma_0\} = \frac{\pi}{l}\int_{-l/2}^{l/2}(\underline{A}_+e^{-ikx} + \underline{A}_-e^{ikx})dx =$$

$$\pi\frac{\sin(kl/2)}{kl/2}(\underline{A}_+ + \underline{A}_-)$$

Since $F^{-1}\{F(\sigma_a)\} = \sigma_a$, substitution of the last two expressions into eq (12) gives an equation for the components $\tilde{\sigma}_+$ and $\tilde{\sigma}_-$ in terms of their inverse FT's.

$$\tilde{\sigma}_\pm = F^{-1}\left\{\pi\frac{\sin(kl/2)}{kl/2}\left[\frac{1}{2}\left(1 \pm \frac{\sin(k\Delta/2)}{k\Delta/2}\right)\underline{A}_+ + \frac{1}{2}\left(1 \mp \frac{\sin(k\Delta/2)}{k\Delta/2}\right)\underline{A}_-\right]\right\} \tag{A8}$$

Equation (A8) gives an indication of the effect of the wave number, k, the gage spacing, Δ, and the gage length, l, on the accuracy. As $k\Delta$ and kl become smaller, the approximations $\tilde{\sigma}_+$ and $\tilde{\sigma}_-$ become closer to the true values σ_+ and σ_-. By assuming that $k\Delta$ and kl are small, which is a necessary condition for acceptable measurements, further simplifications of eq (A8) are obtained by replacing sin functions by low-order series development terms.

$$\frac{\sin(k\Delta/2)}{k\Delta/2} \approx 1 - \frac{k^2\Delta^2}{24}\ldots$$

This gives

$$\tilde{\sigma}_\pm = F^{-1}\left\{\pi\left(1 - \frac{k^2l^2}{24}\right)\left[\left(1 - \frac{k^2\Delta^2}{48}\right)\underline{A}_\pm + \frac{k^2\Delta^2}{48}\underline{A}_\mp\right]\right\}$$

$$= \sigma_\pm + F^{-1}\left\{\pi\frac{k^2}{48}\left[-(\Delta^2 + 2l^2)\underline{A}_\pm + \Delta^2\underline{A}_\mp\right]\right\} \tag{A9}$$

Since $F^{-1}\{\pi\underline{A}_+\} = \sigma_+$ and $F^{-1}\{\pi\underline{A}_-\} = \sigma_-$, the quantities

$$\epsilon_{\rightarrow} = -\frac{k^2(\Delta^2 + 2l^2)}{48}$$

$$\epsilon_{\leftarrow} = \frac{k^2\Delta^2}{48} \tag{A10}$$

have the meaning of relative errors. These errors represent the bias of measurement and are frequency dependent as the wave numbers are frequency dependent.

An Experimental Method for Determining the Dynamic Contact Law

by James F. Doyle

ABSTRACT—An experimental method is investigated whereby the strain response from an impacted beam is sufficient to determine the contacting force. Once the force is known, it is shown how the contact law can be determined. Experimental results for an impacted aluminum beam are demonstrated.

Introduction

The impact resistance of structural materials is very important, especially in such design applications as helicopter rotors or turbine blades. Its need for study is especially acute when using new materials such as fiber-reinforced composites because of their marked susceptibility to hard-object impact damage.

Numerical methods of structural analysis (such as the finite-element method) require that either the forcing history be known or that the dynamic response of both the structure and the impactor be studied simultaneously. In the latter case, it is necessary to have prior experimental knowledge of the contact behavior (or the contact law) between the two bodies. Indeed, an accurate account of this contact behavior becomes the most important step in analyzing the impact response.

The contact law is a relationship between the force and the relative indentation of the impactor and structure,[1] i.e.,

$$F = \mathrm{F}(v_s - v) \tag{1}$$

where v_s is the displacement of the impactor and v is the displacement of the structure. In this form of the law rate effects are incorporated only insofar as they affect F. Thus to obtain the contact law it is necessary to measure the force, the impactor displacement and the structure displacement. This is very difficult to do in dynamic situations, which is why in practice static indentation tests are usually performed.[2]

To develop a fully dynamic test it is necessary to reduce the number of measurements. This can be achieved by invoking particular structural models for the impactor and structure. In the present research:

—the impactor is assumed small so that wave-propagation effects are negligible; then the force and displacement of the impactor are related by

$$m_s \frac{\partial^2 v_s}{\partial t^2} = -F(t) \tag{2}$$

where m_s is the mass of the impactor; and

—the structure is assumed to be a narrow beam of the Bernouilli-Euler type; then the force and beam displacement are related by

$$EI \frac{\partial^4 v}{\partial x^4} + \varrho A \frac{\partial^2 v}{\partial t^2} = P \tag{3}$$

where EI and ϱA are the stiffness and mass per unit length respectively. P is the applied force per unit length.

Obviously other structural models could be used depending on the circumstance. The present modeling is motivated by research on hard-object damage and the fact that the static indentation tests are usually performed on slender strips of the material.

In this manner the force (or any response associated with the beam or impactor) can be considered as the basic unknown. Consequently, during a test only one history need be measured. Possibilities for tests are:

—obtaining the force history by making a force-transducer part of the impactor,[3]

—recording the motion of the impactor by mounting an accelerometer onto it,[4] and

—obtaining the response of the beam by either strain gages or position transducers.

Each of these has its advantages and disadvantages, but in the present research strain gages attached to the beam are chosen primarily because of their insignificant inertia effects and because measurements can be made away from the impact site.

In summary, this paper will report on efforts to determine the force history and contact law from recorded histories of strain.

Basic Scheme

Equation (3) is a complicated differential relation between beam displacement and force. To be able to obtain the force from the strain it is first necessary to solve this equation in an explicit form. This is the single great difficulty of this approach because there are not many known solutions to eq (3).

James F. Doyle (SESA Member) is Associate Professor, Department of Aeronautics and Astronautics, Purdue University, West Lafayette, IN 47906.

Paper was presented at 1983 SESA Spring Meeting held in Cleveland, OH on May 15-20.

Original manuscript submitted: February 10, 1983. Final version received: September 13, 1983.